Scaling and Gridding Geology for SAGD Flow Simulation

Jason A. McLennan

Centre for Computational Geostatistics
Department of Civil & Environmental Engineering
University of Alberta

An important goal of many geostatistical projects is to quantify production uncertainty due to geological uncertainty. For potential SAGD projects, flow simulation is used to convert multiple geostatistical realizations of structure, facies, and petrophysical properties to multiple realizations of production performance parameters; however, flow simulation is computationally expensive. A balance must be met between the high levels of geological detail required to accurately model SAGD flow with the correspondingly high computational price. This balance necessitates scaling the geology modeled by geostatistics to an efficient flow simulation grid. The following paper describes a scaling methodology. The methodology is implemented with different flow simulation gridding schemes to observe the relative effect on SAGD production performance and computational effort.

Introduction

Steam assisted gravity drainage (SAGD) is a popular thermal in-situ heavy oil recovery process in western Canada. The technology was pioneered and developed by Dr. Roger Butler and his collogues at Imperial Oil in the late 1970's. SAGD quickly became a proven technology since then with successful pilot testing at AOSTRA's Underground Test Facility (UTF). Currently, there are over 40 major Oil Sands projects under way or planned.

Figure 1 illustrates the SAGD concept. The procedure is applied to multiple horizontal well pairs up to 1000m long. The upper "injection well" and lower "production well" are nominally parallel and separated by 5m of elevation. To initiate inter-well connectivity, steam is injected through both wells for the first 3 to 6 months. Steam circulation then continues to be injected through the upper injection well only forming a cone shaped steam chamber anchored at the production well. As new reservoir is heated, bitumen lowers in viscosity and flows downward along the outside of the steam chamber boundary via gravity into the production well (Butler, 2004). The primary production performance parameters are the rate oil is produced from the production well (OP_{RATE}) and the amount of steam used relative to oil production or steam-oil-ratio (SOR).

The main objective of using geostatistics for SAGD reservoirs is to quantify the uncertainty in OP_{RATE} and SOR due to geological uncertainty. Figure 2 illustrates this concept. Geological heterogeneity is impossible to predict between conditioning data. The unique true distribution of reservoir properties is and will remain unknown – geological uncertainty is an inherent characteristic of any geological model. Geostatistics can be used to quantify uncertainty through the construction of multiple equally probable realizations of reservoir properties. For each geological realization, flow simulation provides the corresponding OP_{RATE} and SOR response. The difference between production parameter realizations is a measure of production uncertainty.

The expensive computational effort of detailed flow modeling is well known within the petroleum industry. Nevertheless, flow simulation remains an essential link between geological uncertainty and production uncertainty. A balance must then be made between the required level

of geological detail and computer resource demands. This balance is manifested in choosing an appropriate grid resolution. A high resolution grid captures detailed heterogeneity at the price of higher computer resource demand while a low resolution grid runs through flow simulation quickly at the risk of masking heterogeneity important to flow.

Conventional flow simulation studies are usually implemented with upscaled versions of the geology modeled by geostatistics. For most project directives, the resulting savings in computational effort is warranted. Flow simulation for OP_{RATE} and SOR SAGD performance, however, is quite different. Here, the balance between the required level of geological detail and computer resource demand actually involves downscaling the geology. That is, the flow of oil from the steam chamber boundaries to the producer well requires detailed geological heterogeneity to be modeled accurately. Of course, this increased need for geological detail significantly increases the computer resource demand.

SAGD flow simulation requires high performance computers to practically run through the life of a well pair. Efforts to improve the efficiency of these flow simulations on moderate computers without masking important geological heterogeneity has essentially led to different grid designs. For example, smaller cell sizes could be used in the immediate vicinity of the SAGD well pair to capture the important geological and flow detail around the injector and producer wells with larger cells around the outside of the drainage volume to reduce the computational effort.

This paper presents a robust procedure for scaling a geological model of uncertainty to an arbitrary or unstructured flow simulation grid network. The methodology involves three simple steps. The scaling procedure is applied to an example with several flow simulation grid resolutions to demonstrate the process and to investigate the relative effects of the grid on OP_{RATE} and SOR response and computer resource demand.

Scaling Methodology

The scaling process requires a previously constructed geological model of the reservoir. Geostatistics is used to create multiple realizations of structure, facies, porosity, water saturation, and permeability within the entire reservoir volume. An expected cumulative steam chamber volume is then determined around each SAGD well pair of interest. In practice, the scaling methodology described is implemented within each of drainage volume separately.

Three Cartesian grid networks are utilized within each SAGD drainage volume: (1) a geological or geostatistical large-scale or reservoir-scale grid, (2) a fine-scale high resolution geological grid, and (3) an arbitrary flow simulation grid. Table 1 presents an example of these three grid systems. Here, the geostatistical reservoir-scale grid has 25 x 25 x 0.5m cell dimensions, the high resolution grid has 5.0 x 0.4 x 0.4m cell dimensions, and the flow simulation grid has 50 x 2.5 x 2.5m cell dimensions. Larger flow simulation cells are used in the direction parallel to the well pair trajectory to reduce the computational effort without losing significant flow detail. That is, the steam chamber is very likely to propagate along the length of the well pair where steam is explicitly injected. It is the sideways and vertical growth of the steam chamber that significantly effects the production and flow of oil; in these directions smaller cells are used.

There are three general steps to perform within a particular SAGD drainage volume in order to transfer the reservoir-scale geology to the arbitrary-scale flow simulation geology: (1) extract the geostatistical model, (2) downscale the extracted geology, and (3) upscale the downscaled geology to the flow simulation grid. Each step involves at least one of the grid networks in Table 1. These three steps are now described in detail.

A preliminary calculation of all the grid network cell centroids is required. The first step then involves extracting the geology from the large-scale or reservoir-scale model centroids that are closest to the flow simulation grid cell centroids. The geology from those reservoir-scale cells with centroids outside the SAGD drainage volume are not extracted. The result is multiple realizations of structure, facies, porosity, water saturation, and permeability at each of the flow simulation grid cell centroids within the drainage volume.

The extracted reservoir-scale geology in the previous step is then used to downscale to the high resolution grid resolution within the drainage volume. This step ensures there are multiple geological data within the smallest anticipated flow simulation grid cell boundary. A geostatistical re-simulation procedure (sequential indicator simulation for facies and sequential Gaussian simulation for porosity, water saturation, and permeability) conditioned by the extracted geology is used in the downscaling process. The same reservoir-scale variography is used. The result is multiple high resolution geological realizations within the drainage volume.

The high resolution geology created in the previous step is then upscaled to an arbitrary flow simulation grid network. The most common facies, the arithmetic average porosity and water saturation, and the geometric average permeability are calculated to populate the flow simulation grid network. The flow simulation grid can be any type of arbitrary or unstructured grid as long as there are multiple fine-scale geological locations contained within the boundaries of the smallest flow simulation cell.

This scaling procedure is implemented on a number of different regular and irregular flow simulation grid systems to investigate how sensitive the OP_{RATE} and SOR flow response variables and computer resource demand are to the grid network.

Implementation and Results

A suite of 100 geological realizations of facies, porosity, water saturation, and permeability are constructed within a 2 x 2 x 0.1km reservoir volume. Figure 3 shows the aerial view of the reservoir with four exploratory coreholes located in each corner of the reservoir as well as a particular 800 x 150 x 0.1m SAGD drainage volume outline of interest. The geostatistical realizations are synthetically created to mimic a high quality net pay interval. Uncertainty in the top and bottom surfaces is not considered. There are 5 facies types: sand, breccia, interbedded sand, interbedded shale, and shale. The porosity, water saturation, and permeability variables are modeled separately within each facies.

Several different flow simulation grid networks are considered in this work. Table 2 summarizes 13 different regular grid networks corresponding to 1 base case and 4 sensitivities for each of the 3 *X*, *Y*, and *Z* directions. The number, minimum, and size in each of the coordinate directions and total number of cells are all tabulated. Table 3 presents 2 different irregular grid networks corresponding to different levels of grid refinement (L1, L2, …) in the *Y* direction. The scaling results will be presented for the base case only. The computer resource demand and performance flow simulation results for all 15 flow simulation grid cases will then be presented.

Table 1 shows the large-scale reservoir grid and high resolution grid used for all 15 gridding scenarios as well as the flow simulation grid for the base case. The 50^{th} geological realization is extracted to the 50.0 x 2.5 x 2.5m flow simulation grid cell centroids (38,400 total) within the drainage volume. Figure 4 shows the distribution of each extracted variable. This data is then used to downscale the geology to the high resolution 5.0 x 2.5 x 2.5m grid system (20,000,000 total). Figure 5 shows a central *XY* cross sectional view through the downscaled geology within the drainage volume. This fine-scale geology is then upscaled to the 50.0 x 2.5 x 2.5m flow

simulation grid cells. Figure 6 shows the distribution of upscaled geology, compare with Figure 4. This downscaling and upscaling process is repeated for each flow simulation grid network.

Flow simulation is performed using the upscaled geology on each of the 15 flow simulation grid networks. A single 500m long well pair is used. The production and injection well are located 20 and 25m from the base of the reservoir, respectively. The project life is 6.5 years including a 6 month hot finger stimulation startup, a 2 year high pressure phase, a 2 year low pressure phase, and a 2 year blowdown phase. The flow simulations produce OP_{RATE} and SOR response profiles. The cumulative OP_{RATE} and SOR for the base case are shown in Figure 7. Figure 8 shows the cumulative steam chamber (100°C iso-surface) during the low pressure phase of operation.

The results of the example are summarized in Figures 9 through 11 showing the cumulative OP_{RATE} and SOR results for the *X*, *Y*, and *Z* grid sensitivities, Figure 12 showing the cumulative OP_{RATE} and SOR results for *Y* direction grid refinement, and Table 4 showing the time of each flow simulation run. These results are now interpreted.

Interpretation

There are no history data available for this particular example, that is, there is no truth to compare the sensitivity studies to; however, there are a number of simple and important observations that can be made between the scenarios investigated in this paper.

From Figure 9, it seems that a decrease in the *X* cell dimension is beneficial in terms of cumulative OP_{RATE} and SOR. For example, for 16m cell lengths, the SOR improves (decreases) by approximately 0.25 from that from the 50m cell length base case. From Table 4, this is associated with a relatively low increase of approximately 4.5 hours in computational effort. Without history data, it is impossible to tell if this improvement in production performance is realistic. Nevertheless, the improvement may warrant at least trying higher discretizations along the well pair in practice and observing the relative history matches.

Figure 10 and Table 4 show that the highest *Y* direction grid resolution comes at a significant computational price increase of 12.5 hours with little production performance difference relative to the base case. For Case 07, the increased computational effort is only 1.25 hours and there is virtually no difference in production performance. The low *Y* resolution production profiles are somewhat unrealistic since heat transfer becomes very difficult through large sideways distances. In practice, the *Y* resolution should not be chosen too high due to computational effort nor too low due to unrealistic heat transfer and steam chambers.

Figure 11 and Table 4 show that the *Z* grid resolution is fairly inconsequential to production performance but very significant in terms of computational effort. However, the 4m *Z* cell length seemed to have improved the OP_{RATE} and SOR values. The highest resolution scenario caused unrealistically tall and skinny steam chambers since heat transfer was preferred through the small vertical cell distances. In practice, it is recommended to use a *Z* cell length that produces realistic steam chamber shapes.

Finally, Figure 12 and Table 4 suggest that the effort involved in applying several levels of *Y* direction refinement results in significantly higher computer resource demands with virtually no difference in SAGD production performance.

References

Butler, R., 2004. *Thermal Recovery of Oil and Bitumen*, GravDrain Inc., Calgary, Alberta, 1997.

Computer Modeling Group (CMG). *STARS 2004.12 User's Guide*, CMG, Calgary, Alberta, 2004.

		GRID SYSTEM		
		Geostatistical	High Resolution	Flow Simulation
X	number	32	160	16
	minimum	12.50	2.50	25.00
	size	25.00	5.00	50.00
Y	number	8	500	60
	minimum	12.50	0.20	1.25
	size	25.00	0.40	2.50
Z	number	200	250	40
	minimum	0.25	0.20	1.25
	size	0.50	0.40	2.50

Table 1 – Scaling Grid Networks. Three different grid networks are needed to downscale and upscale the geological model from geostatistics to flow simulation within a particular SAGD drainage volume.

	DIRECTION	NUMBER	MINIMUM	SIZE	MINEDGE	MAXEDGE	TOTAL
BASE CASE (01)	X	16	25.00	50.00	0.00	800.00	38,400
	Y	60	1.25	2.50	0.00	150.00	
	Z	40	1.25	2.50	0.00	100.00	
CASE 02	DIRECTION	NUMBER	MINIMUM	SIZE	MINEDGE	MAXEDGE	TOTAL
	X	50	8.00	16.00	0.00	800.00	120,000
	Y	60	1.25	2.50	0.00	150.00	
	Z	40	1.25	2.50	0.00	100.00	
CASE 03	DIRECTION	NUMBER	MINIMUM	SIZE	MINEDGE	MAXEDGE	TOTAL
	X	32	12.50	25.00	0.00	800.00	76,800
	Y	60	1.25	2.50	0.00	150.00	
	Z	40	1.25	2.50	0.00	100.00	
CASE 04	DIRECTION	NUMBER	MINIMUM	SIZE	MINEDGE	MAXEDGE	TOTAL
	X	10	40.00	80.00	0.00	800.00	24,000
	Y	60	1.25	2.50	0.00	150.00	
	Z	40	1.25	2.50	0.00	100.00	
CASE 05	DIRECTION	NUMBER	MINIMUM	SIZE	MINEDGE	MAXEDGE	TOTAL
	X	8	50.00	100.00	0.00	800.00	19,200
	Y	60	1.25	2.50	0.00	150.00	
	Z	40	1.25	2.50	0.00	100.00	
CASE 06	DIRECTION	NUMBER	MINIMUM	SIZE	MINEDGE	MAXEDGE	TOTAL
	X	16	25.00	50.00	0.00	800.00	192,000
	Y	300	0.25	0.50	0.00	150.00	
	Z	40	1.25	2.50	0.00	100.00	
CASE 07	DIRECTION	NUMBER	MINIMUM	SIZE	MINEDGE	MAXEDGE	TOTAL
	X	16	25.00	50.00	0.00	800.00	64,000
	Y	100	0.75	1.50	0.00	150.00	
	Z	40	1.25	2.50	0.00	100.00	
CASE 08	DIRECTION	NUMBER	MINIMUM	SIZE	MINEDGE	MAXEDGE	TOTAL
	X	16	25.00	50.00	0.00	800.00	19,200
	Y	30	2.50	5.00	0.00	150.00	
	Z	40	1.25	2.50	0.00	100.00	

	DIRECTION	NUMBER	MINIMUM	SIZE	MINEDGE	MAXEDGE	TOTAL
CASE 09	X	16	25.00	50.00	0.00	800.00	9,600
	Y	15	5.00	10.00	0.00	150.00	
	Z	40	1.25	2.50	0.00	100.00	
CASE 10	DIRECTION	NUMBER	MINIMUM	SIZE	MINEDGE	MAXEDGE	TOTAL
	X	16	25.00	50.00	0.00	800.00	192,000
	Y	60	1.25	2.50	0.00	150.00	
	Z	200	0.25	0.50	0.00	100.00	
CASE 11	DIRECTION	NUMBER	MINIMUM	SIZE	MINEDGE	MAXEDGE	TOTAL
	X	16	25.00	50.00	0.00	800.00	96,000
	Y	60	1.25	2.50	0.00	150.00	
	Z	100	0.50	1.00	0.00	100.00	
CASE 12	DIRECTION	NUMBER	MINIMUM	SIZE	MINEDGE	MAXEDGE	TOTAL
	X	16	25.00	50.00	0.00	800.00	24,000
	Y	60	1.25	2.50	0.00	150.00	
	Z	25	2.00	4.00	0.00	100.00	
CASE 13	DIRECTION	NUMBER	MINIMUM	SIZE	MINEDGE	MAXEDGE	TOTAL
	X	16	25.00	50.00	0.00	800.00	19,200
	Y	60	1.25	2.50	0.00	150.00	
	Z	20	2.50	5.00	0.00	100.00	

Table 2 – Regular Flow Simulation Grid Networks. Thirteen different regular flow simulation grid networks are investigated. This includes one base case and 4 sensitivities in each of 4 coordinate directions.

	DIRECTION	NUMBER	MINIMUM	SIZE	MINEDGE	MAXEDGE	TOTAL
CASE 14	X	16	25.00	50.00	0.00	800.00	128,000
	Y (L1)	50	0.50	1.00	0.00	50.00	
	Y (L2)	100	50.25	0.50	50.00	100.00	
	Y (L3)	50	100.50	1.00	100.00	150.00	
	Z	40	1.25	2.50	0.00	100.00	
CASE 15	DIRECTION	NUMBER	MINIMUM	SIZE	MINEDGE	MAXEDGE	TOTAL
	X	16	25.00	50.00	0.00	800.00	70,400
	Y (L1)	5	2.50	5.00	0.00	25.00	
	Y (L2)	10	26.25	2.50	25.00	50.00	
	Y (L3)	10	50.50	1.00	50.00	60.00	
	Y (L4)	60	60.25	0.50	60.00	90.00	
	Y (L5)	10	90.50	1.00	90.00	100.00	
	Y (L6)	10	101.25	2.50	100.00	125.00	
	Y (L7)	5	127.50	5.00	125.00	150.00	
	Z	40	1.25	2.50	0.00	100.00	

Table 3 – Irregular Flow Simulation Grid Networks. Two different irregular flow simulation grid networks are investigated. Case 14 involves 3 levels of *Y* grid refinement and Case 15 involves 7 levels of *Y* grid refinement.

TIME (MINUTES)	
BASE CASE (01)	1:15:44
CASE 02	5:57:07
CASE 03	3:15:22
CASE 04	0:36:00
CASE 05	0:25:23
CASE 06	13:45:46
CASE 07	2:31:36
CASE 08	0:18:30
CASE 09	0:06:23
CASE 10	13:54:59
CASE 11	4:01:00
CASE 12	0:37:45
CASE 13	0:30:00
CASE 14	12:20:00
CASE 15	9:54:21

Table 4 – Computer Resource Demand. The run time of each flow simulation gridding scenario.

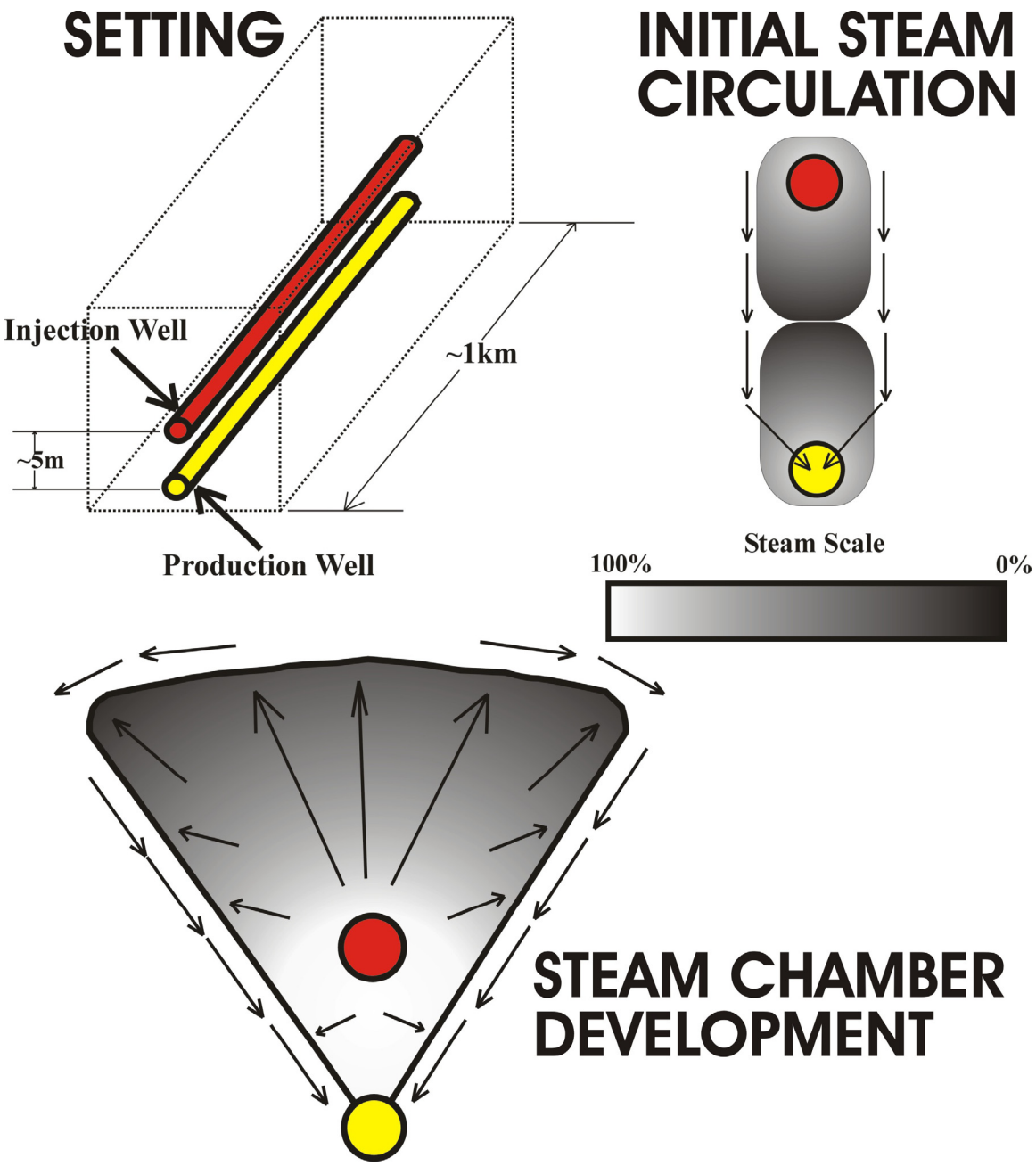

Figure 1 – Steam Assisted Gravity Drainage (SAGD). The SAGD process is applied to horizontal well pairs (top left). Steam is first injected through both the injection and production well to initiate a steam chamber connecting the reservoir between wells. Steam circulation then continues in the injection well only forming a cone shaped steam chamber anchored at the production well (bottom). New bitumen is continually heated and drained along the outside of the steam chamber via gravity.

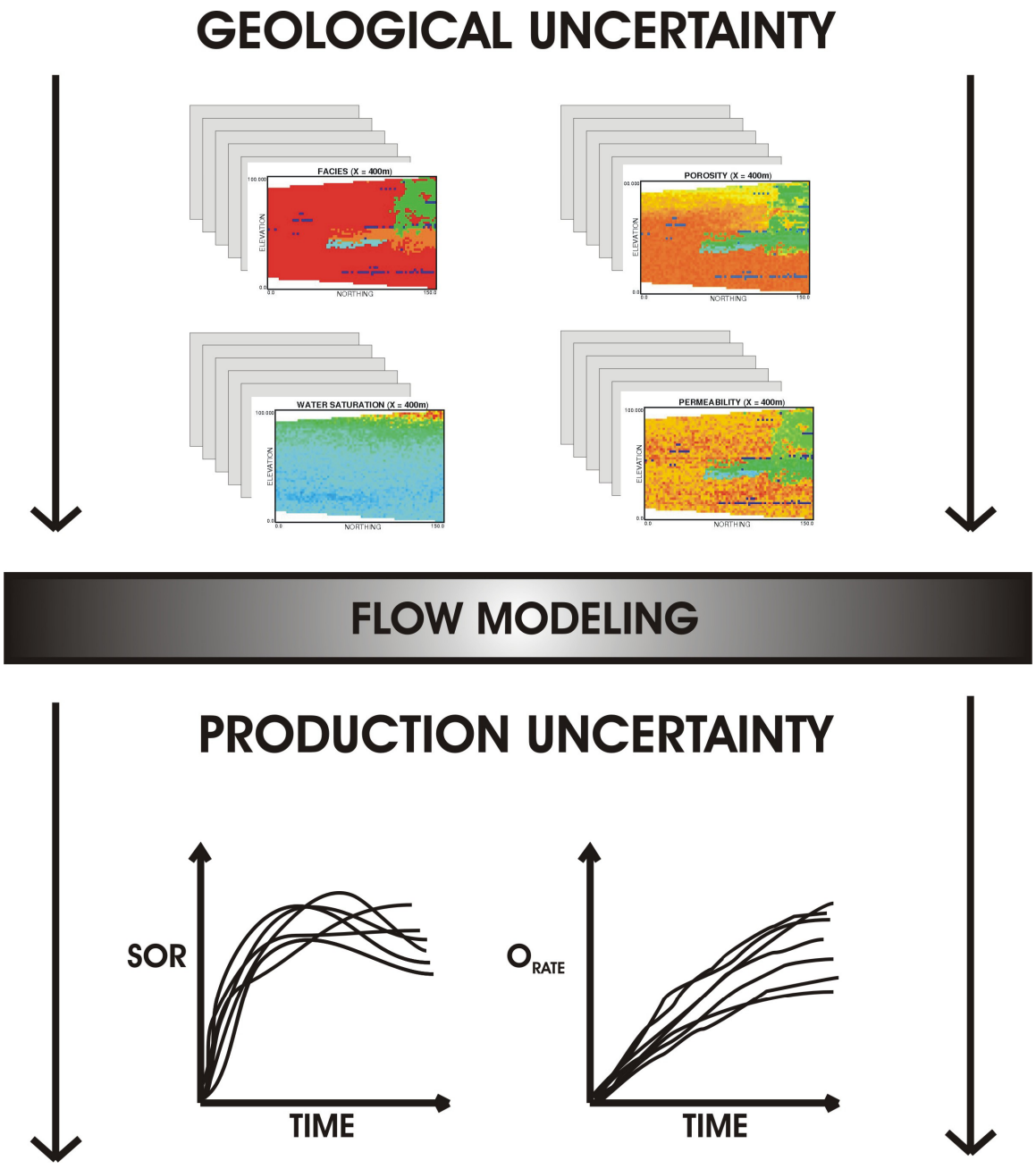

Figure 2 – Uncertainty. Geostatistics is used to quantify geological uncertainty as the difference between multiple equally probable realizations of facies, porosity, water saturation, and permeability. Flow modeling provides the SAGD response (SOR and ORATE) for each realization. The difference between these responses is then a measure of production uncertainty.

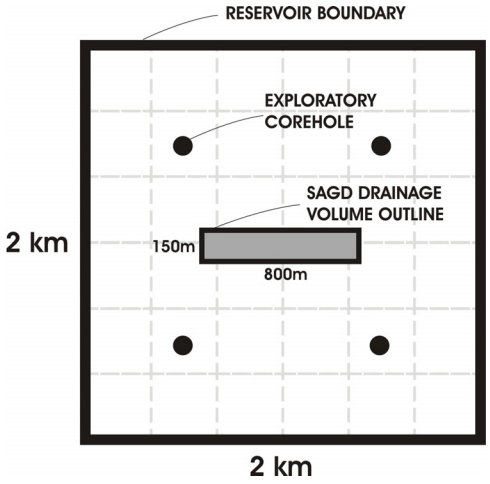

Figure 3 – Example Setting. A schematic of the example setting showing the aerial reservoir and drainage volume extents (the reservoir is 100m thick) as well as four conditioning wells for subsequent geostatistical simulation.

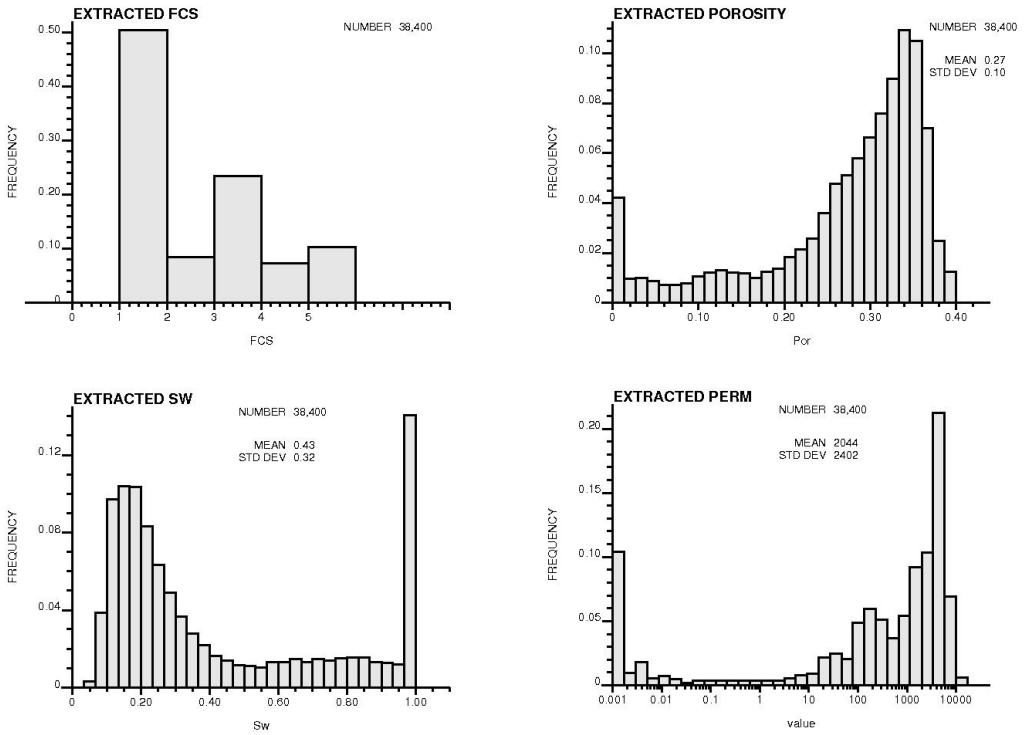

Figure 4 – Extracted Geology. The distribution of facies, porosity, water saturation, and permeability extracted from the reservoir-scale geological model to the flow simulation grid.

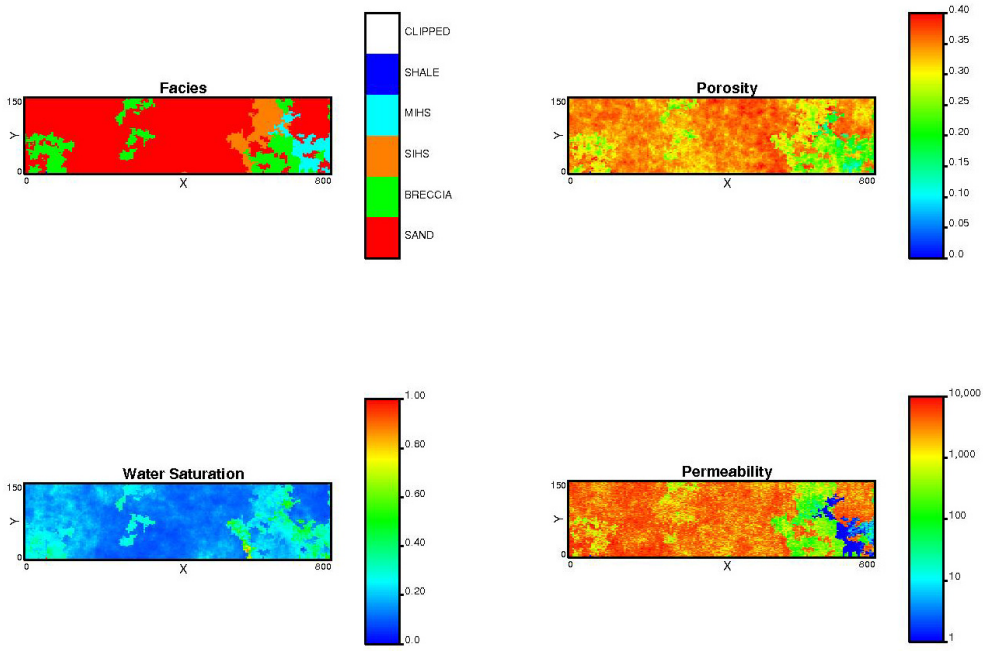

Figure 5 – Downscaled Geology. A central *XY* slice through the high resolution model of facies, porosity, water saturation, and permeability re-simulated using the extracted geology.

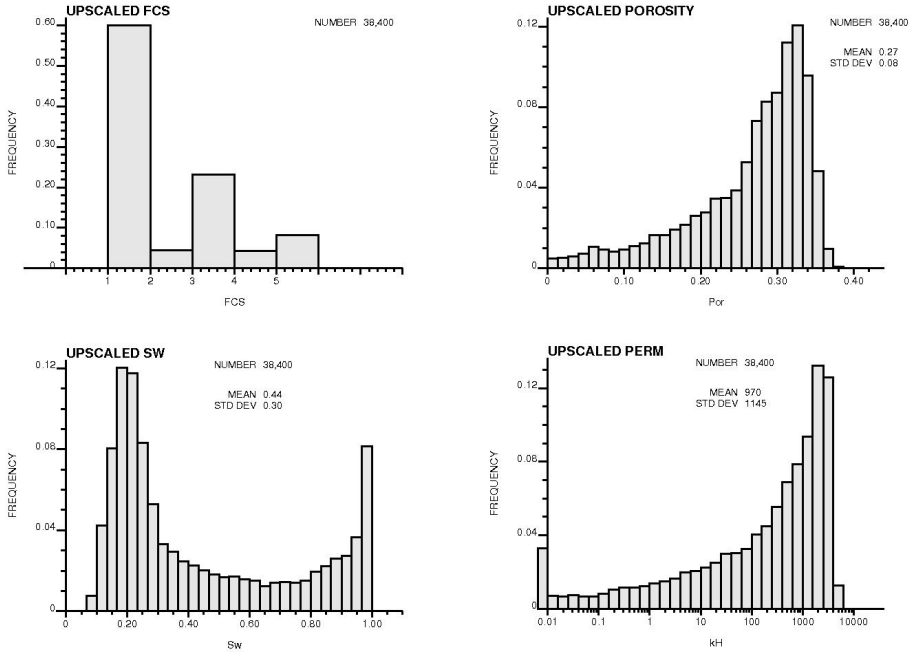

Figure 6 – Upscaled Geology. The distribution of facies, porosity, water saturation, and permeability upscaled from the high resolution geological model to the flow simulation grid.

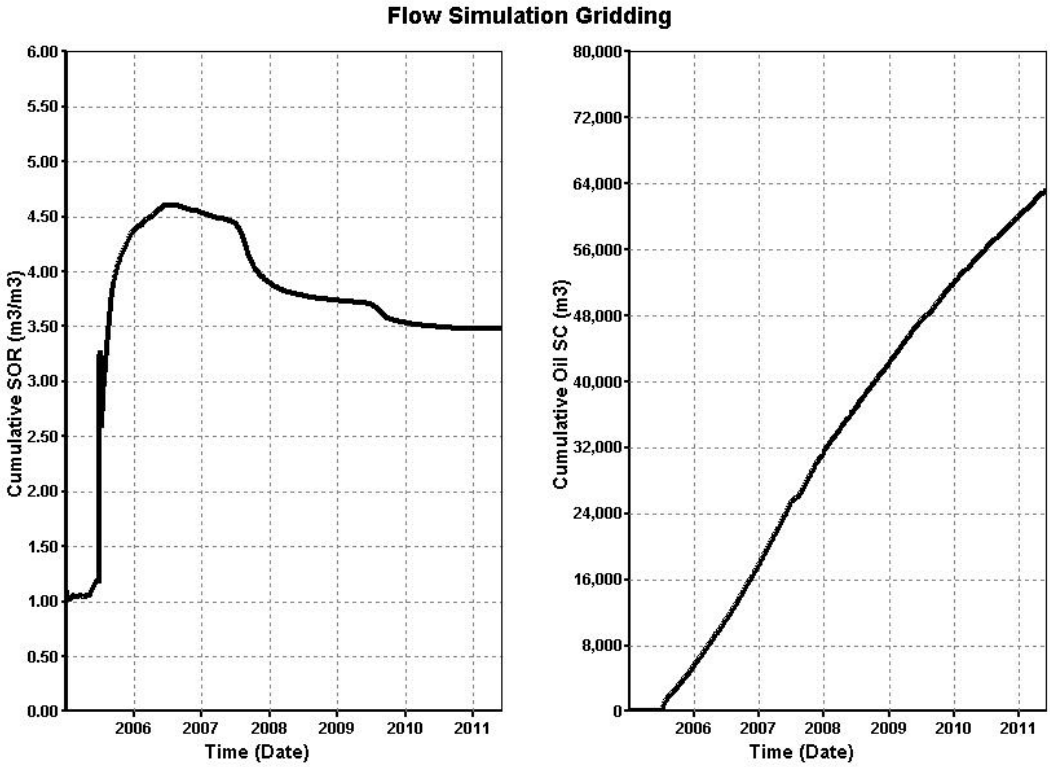

Figure 7 – Base Case Flow Results. The cumulative O_{RATE} and SOR profiles for the base case flow simulation grid.

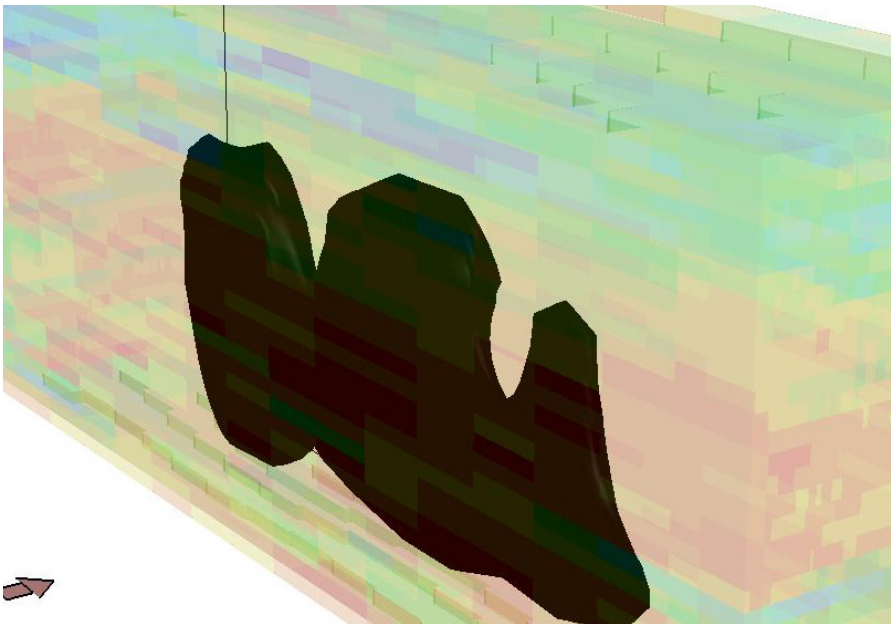

Figure 8 – Base Case Steam Chamber. The cumulative steam chamber (100°C iso-surface) for the base case flow simulation grid scenario.

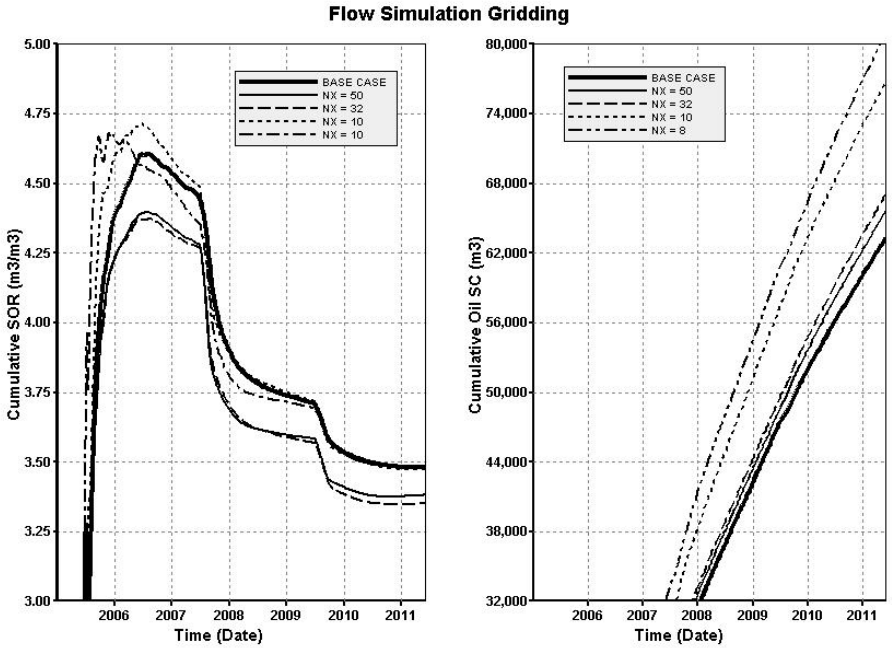

Figure 9 – *X* Direction Flow Results. The cumulative O_{RATE} and SOR profiles for the *X* grid flow simulation scenarios.

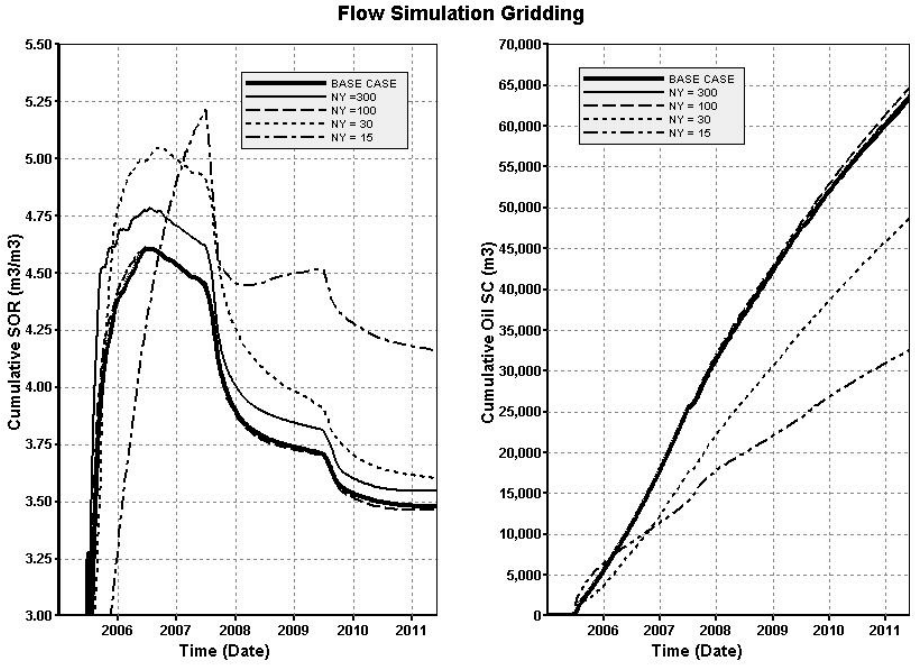

Figure 10 – *Y* Direction Flow Results. The cumulative O_{RATE} and SOR profiles for the *Y* grid flow simulation scenarios.

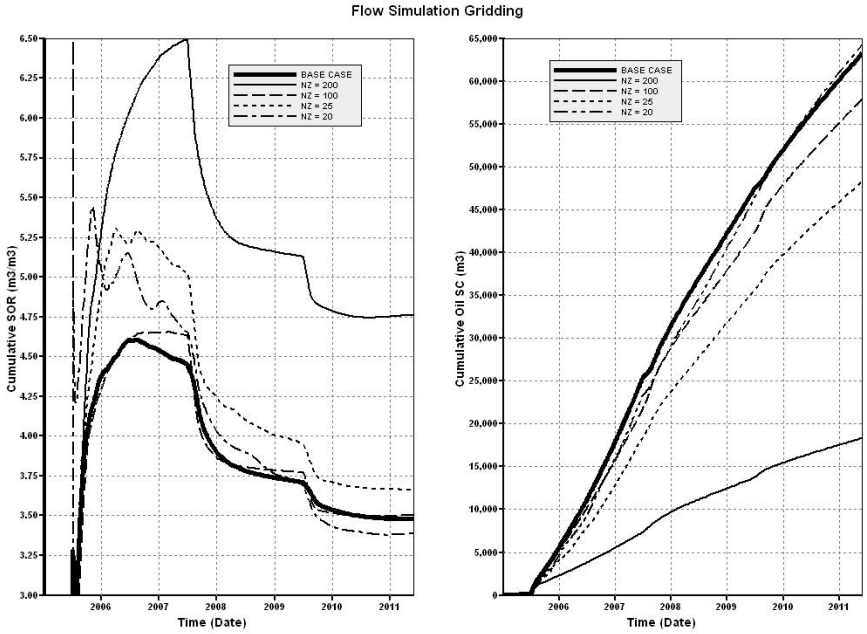

Figure 11 – *Z* Direction Flow Results. The cumulative O_{RATE} and SOR profiles for the *Z* grid flow simulation scenarios.

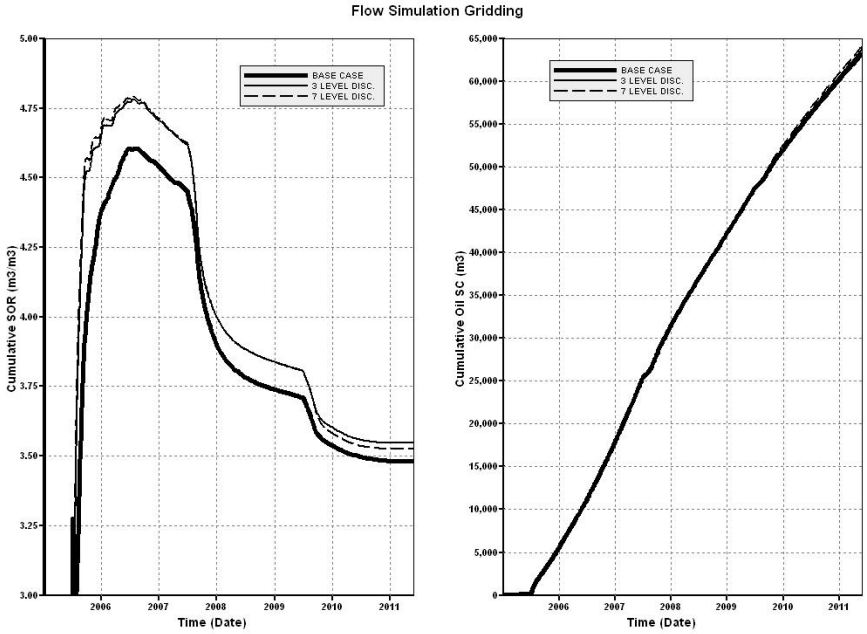

Figure 12 – *Y* Direction Discretization Flow Results. The cumulative O_{RATE} and SOR profiles for the *Y* direction grid refinement flow simulation scenarios.